

**Pop-in effect as homogeneous nucleation of dislocations during nanoindentation**

D. Lorenz, A. Zeckzer, U. Hilpert, and P. Grau

*Fachbereich Physik, Friedemann-Bach-Platz 6, Martin-Luther-Universität, D-06108 Halle, Germany*

H. Johansen

*Max-Planck-Institut für Mikrostrukturphysik, Weinberg 2, D-06120 Halle, Germany*

H. S. Leipner\*

*Interdisziplinäres Zentrum für Materialwissenschaften, Hoher Weg 8, Martin-Luther-Universität, D-06120 Halle, Germany*

(Received 23 October 2002; published 5 May 2003)

Using advanced depth-sensitive hardness measurements, the homogenous nucleation of dislocations has been observed in dislocation-free single crystals. This process is related to a sudden displacement jump in the force-displacement curve. The mechanical stress for the set-in of this pop-in effect has been estimated with the Hertzian elastic contact theory. Experimental results of dislocation loop nucleation show good agreement with the continuum theory of dislocations. Electron microscopy provides a direct proof of dislocation nucleation during nanoindentation.

DOI: 10.1103/PhysRevB.67.172101

PACS number(s): 61.72.Lk, 81.40.Lm

**I. INTRODUCTION**

Nanoindentation is an excellent tool to determine mechanical properties on a local scale. Moreover, the topography of the residual impression can be studied in the atomic-force-microscopy mode by the same tip used for the indentation.<sup>1</sup> The physical background of the indentation load-displacement behavior of single crystals on a nanometer scale has been a matter of intensive experimental<sup>2-4</sup> and theoretical<sup>5-7</sup> studies. The load-displacement curves obtained by nanoindentation may show discontinuities at load levels below 1 mN, which characterize a sharp transition from pure elastic to plastic deformation. It has been related to homogeneous defect generation and surface roughness in recent model experiments.<sup>8</sup> The role of dislocation generation and slip has been discussed in comparison to structural transformations.<sup>9</sup> Microscopical investigations have been used to prove defect generation during nanoindentation.<sup>10-12</sup> The basic process in a broad range of materials (metals, ceramics, semiconductors, ionic crystals) seems to be the homogeneous nucleation of dislocations.<sup>13,14</sup>

During depth-sensitive hardness measurements a diamond indenter is penetrating the sample under continuous registration of force  $F$  and penetration depth  $h$ . The mean contact pressure  $p_m$  increases according to the Hertzian contact theory<sup>15</sup> with the square root of the penetration depth,

$$p_m = \frac{F}{\pi a^2} = \frac{4}{3\pi} \tilde{E} \sqrt{\frac{h}{R}}.$$

Here  $2a$  is the diameter of the contact circle,  $\tilde{E}$  the effective elastic modulus, and  $R$  the radius of the indenter tip, which is regarded as a sphere. The strength of the material restricts therefore the feasible maximum contact pressure. The very high stress beneath the indenter may result in phase transitions,<sup>16,17</sup> crack formation,<sup>18</sup> or homogenous dislocation nucleation.<sup>13,14</sup> In the present paper, the conditions of the latter effect are investigated in detail.

The shear stress  $\tau$  necessary for homogeneous dislocation nucleation can be calculated from the elastic self-energy stored in a dislocation loop.<sup>19</sup> From the equilibrium between the elastic energy and the work necessary to form a dislocation loop of the radius  $r$  in an isotropic medium,

$$\tau = \frac{2-\nu}{1-\nu} \frac{Gb}{4\pi r} \left( \ln \frac{4r}{r_0} - 2 \right).$$

Thermal contributions and the possible formation of a stacking fault are neglected.  $G$  is the shear modulus,  $b$  the magnitude of the Burgers vector,  $\nu$  Poisson's ratio, and  $r_0$  the inner cutoff radius. The maximum of the relation  $\tau = \tau(r)$  is the critical stress  $\tau_c$  at the critical loop radius  $r_c$  for dislocation nucleation,

$$\tau_c \approx \frac{Gb}{2\pi r_c} \approx \frac{G}{10}. \quad (1)$$

The maximum shear stress (according to the Tresca criterion)  $\tau_T$  beneath a spherical indenter can be expressed as a function of the mean contact pressure or the indentation force and the penetration depth  $h$  at known tip radius  $R$  of the indenter,<sup>15</sup>

$$\tau_T = 0.465 p_m = 0.465 \frac{4\tilde{E}}{3\pi} \sqrt{\frac{h}{R}}. \quad (2)$$

The effective elastic modulus  $\tilde{E}$  is obtained from Young's modulus  $E$  and Poisson's ratio of the sample and those values of the indenter material (diamond:  $E_i = 1141$  GPa,  $\nu_i = 0.07$ ),

$$\frac{1}{\tilde{E}} = \frac{1-\nu^2}{E} + \frac{1-\nu_i^2}{E_i}.$$

It follows from the analysis of the elastic stress field that the maximum hydrostatic pressure is, depending on Pois-

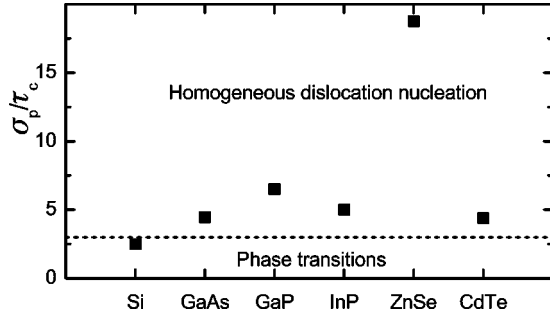


FIG. 1. Ratio between the minimum hydrostatic pressure of phase transitions,  $\sigma_p$  (Ref. 16), and the stress of homogeneous dislocation nucleation in different materials. The ratio of the maximum hydrostatic pressure and the maximum shear stress calculated from contact theory of isotropic elastic bodies amounts to 2.8 for  $\nu = 0.35$ , and it is indicated as a dashed line.

son's ratio, about 2–3 times higher than the maximum shear stress  $\tau_T$ . For  $\nu = 0.35$ , the ratio of the maximum hydrostatic pressure and the maximum shear stress calculated from contact theory of elastic bodies amounts to 2.8. This value is indicated as a dashed line in Fig. 1. Furthermore, the ratio between the hydrostatic pressure required for phase transitions<sup>16</sup> and the critical shear stress of homogenous dislocation nucleation [Eq. (1)] is compared for different semiconductor single crystals in this figure. It is evident that this value is smaller than 2.8 in Si, and therefore phase transitions are initiated before  $\tau_c$  is reached. Consequently, the pop-in effect in Si cannot be described by a dislocation model.

Homogenous dislocation nucleation is only possible if no mobile dislocations already exist in the sample close to the indenter. The number of dislocations,  $N$ , likely to be activated can be calculated as the product of the contact area between sample and indenter at the depth  $h_j$  where the pop-in jump sets in and the dislocation density  $\rho$  of the material,

$$N = \rho \pi R h_j.$$

It should be noted that  $N$  is a mere statistical quantity. For  $N \geq 1$ , we assume that existing dislocations inside the stressed area take part continuously in plastic deformation and no sudden displacement jump occurs. Below  $N = 0.01$ , the pop-in effect has been observed experimentally with high probability.

Assuming  $\tilde{E} \approx 3G$  and substituting the critical shear stress from Eq. (1) into Eq. (2) for  $h = h_j$ , the pop-in penetration depth depends only on the tip radius,

$$h_j \approx 0.03R. \quad (3)$$

As a result of this approximation, the number of existing dislocations likely to be activated before the pop-in effect appears can be written as

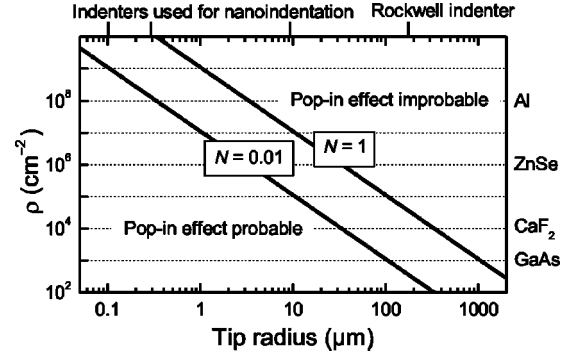


FIG. 2. Occurrence of the pop-in effect as a function of the tip radius  $R$  and the density of dislocations present in the material,  $\rho$ .  $N$  is the number of dislocations likely to be activated within the indenter stress field. The materials studied are indicated at their typical dislocation densities. The indenter radii used are marked at the upper scale.

$$N \approx 0.09\rho R^2. \quad (4)$$

This equation is illustrated in Fig. 2 in a log–log plot of the dislocation density versus the tip radius for the parameter  $N = 1$  and  $N = 0.01$ , respectively. With a high degree of certainty, the pop-in effect will not appear if the dislocation density is higher than  $10^9 \text{ cm}^{-2}$  for an indenter tip radius  $\geq 1 \mu\text{m}$ . The pop-in effect is not expected for indentations with an large indenter, such as a Rockwell indenter, even if the dislocation density is low. This conclusion is confirmed by measurements with different indenters and materials, indicated on the upper and right axes of Fig. 2.

## II. EXPERIMENT

Depth-sensitive hardness measurements were carried out at room temperature under constant loading and unloading rates using the MTS Systems Nanoindenter II. For the materials tested, a variation of the loading rate within the range 1–3000  $\mu\text{N/s}$  did not show any significant influence on the characteristic values measured for the pop-in effect. A loading rate of 1  $\mu\text{N/s}$  was chosen to analyze the load-displacement curves with high accuracy in acceptable time.

The indenters used for the experiments were selected with respect to significantly different tip radii ranging from 0.1 to 10  $\mu\text{m}$  (Fig. 2), as measured by atomic force microscopy. In order to obtain universally valid results, a broad range of materials was investigated. Single-crystalline metals (Al, Ni, W), semiconductors (Si, GaAs, InP, epitaxial ZnSe on GaAs), and ionic crystals (BaF<sub>2</sub>, CaF<sub>2</sub>) were studied in different surface orientations. For the preparation of the bulk semiconductors and ionic crystals, standard polishing procedures were used. In addition, cleavage faces were studied.

Panchromatic cathodoluminescence (CL) images were taken at 77 K in a JEOL JSM 6400 scanning electron microscope operating at 8 kV. With this technique, dislocations in semiconductors can be easily recognized, because they can act as centers of the nonradiative recombination of excess carriers (dark contrast) or as centers of radiative recombination (bright contrast against the matrix luminescence).

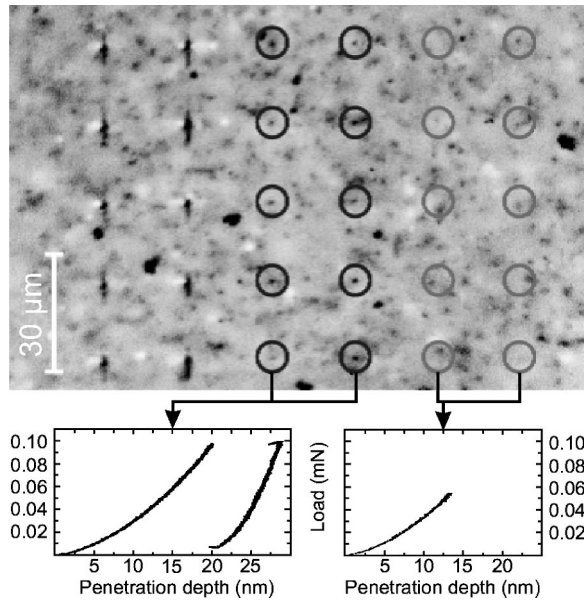


FIG. 3. CL image of a ZnSe layer with indentations ( $R = 0.1 \mu\text{m}$ ) with loads of 0.05 mN (two columns on the right), 0.1 mN (two middle columns), and 2 mN (two columns on the left). The low-load indentation sites are marked by circles. Typical load-displacement curves of the 0.05 and the 0.1 mN indentations, respectively, are shown below.

The formation of dislocations at indentations was studied by transmission electron microscopy in diffraction contrast, carried out with a JEM 1000 microscopy operating at 1 MV.

### III. RESULTS AND DISCUSSION

Figure 3 shows a CL image of indentations in a 4.2- $\mu\text{m}$ -thick epitaxial layer of (001) ZnSe/GaAs. The density of in-grown dislocations amounts to  $2 \times 10^6 \text{ cm}^{-2}$ . In accordance with Fig. 2, it is low enough for the appearance of the pop-in effect.

A set of indentations produced with different maximum loads is visible. The indentations are marked by circles for the low-load experiments. In the CL image, dark contrasts appear at the indentation sites for maximum loads  $\geq 0.1$  mN, indicating the nucleation of dislocations. More extended dislocation contrasts are to be seen at the 2 mN indentations in the two columns on the left. There, bright and dark CL contrasts can be distinguished. In accordance to earlier work on dislocations in II-VI compound semiconductors, these contrasts can be attributed to the different core structure of polar dislocations known as  $\alpha$  and  $\beta$  dislocations, respectively.<sup>20</sup>

The pop-in effect appears in this case and also for the indentations in the middle columns with a maximum load of 0.1 mN, as can be seen in the load-displacement curves. Typical curves are shown in Fig. 3. For all indentations in the two middle columns of Fig. 3, there is a scatter in the pop-in load ranging from 0.06 to 0.14 mN. Before the pop-in effect appears, all loading and unloading curves are identical. This behavior is found for maximum loads of 0.05 mN applied for the indentations in the two columns on the right in Fig. 3.

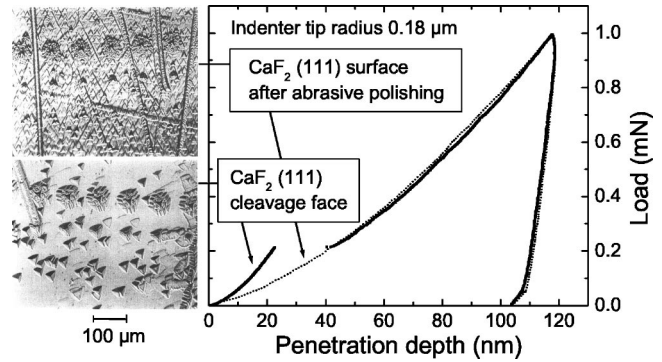


FIG. 4. Load-displacement curve measured during indentation of a (111) cleavage face of  $\text{CaF}_2$  compared to that of a (111) surface after grinding (dotted line). The micrographs on the left show etched dislocations present in the sample and those introduced during indentation. The rows of indentations with 100, 10, and 1 mN are visible.

The deformation is pure elastic. The load-displacement curves registered exhibit no displacement jump for these indentations with maximum load of 0.05 mN. The pop-in effect is connected with the set-in of plastic deformation, and the loading and unloading curves are different. In contrast, no cathodoluminescence contrasts in addition to the in-grown defects appear regularly at the positions of the 0.05 mN indentations, indicating that no fresh dislocations are nucleated.

Transmission electron microscopy (TEM) could directly show the dislocation rosette formed at indentations in GaAs shortly after the pop-in jump.<sup>11</sup> The dislocation loops visible in TEM are the result of dislocation generation and multiplication. The critical stress of dislocation motion is orders of magnitude smaller than the critical stress of homogeneous dislocation nucleation. In this way, plastic deformation can proceed easily after dislocation generation by conventional multiplication processes.

The influence of preexisting dislocations on the load-displacement curve is demonstrated in Fig. 4. While the displacement jump occurs during indentation of the cleavage plane of the  $\text{CaF}_2$  sample, it does not occur on a (111) surface after grinding. In the latter case, the elastic-plastic deformation can proceed via mobilization and multiplication of the dislocations introduced by the pretreatment, and the pop-in effect does not occur. After the pop-in jump, the load-displacement curves are identical. This means that the plastic deformation beneath the indenter is comparable for both surfaces. The dislocations present in the samples and generated during nanoindentations are visible in the micrographs of Fig. 4 after etching in a solution of  $5 \text{ HNO}_3 + 1 \text{ HClO}_3 + 5 \text{ H}_2\text{O}$  for 15 min.

Figure 5 shows  $\tau_T$  calculated at  $h_j$  in comparison to  $\tau_c$  from Eq. (1) for different single crystals and indenters. One can see that  $\tau_T$  determined from the indentation experiment at the pop-in jump is always very close to or higher than the theoretical critical generation stress of dislocations. The higher values can be explained by the fact that the resolved shear stress acting in a particular slip system is always

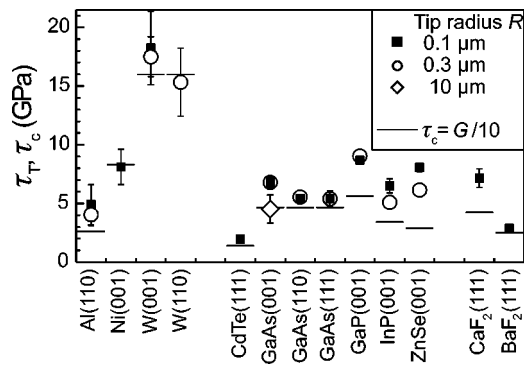


FIG. 5. Tresca stress  $\tau_T$  for the appearance of the pop-in effect at different tip radii and dislocation nucleation stress  $\tau_c$  in different materials.

smaller than or equal to the Tresca stress. Only for special orientations of the slip plane and glide direction does the resolved shear stress equal the Tresca stress. This explains the variation of the measured  $\tau_T$  for different crystal orien-

tations. To describe this effect in more detail, calculations which take into account the anisotropy of the materials are being carried out.

#### IV. CONCLUSIONS

The appearance of the pop-in effect in different single crystals can be interpreted as a manifestation of the homogeneous nucleation of glissile dislocation loops. Conventional multiplication processes of these loops permit strong local plastic deformation. The jump in the load-displacement curves is thus the transition from pure elastic to elastic-plastic deformation, if no dislocations already present in the sample can be activated. The analysis of the elastic part of the load-displacement curve with the quasi-isotropic description as Hertzian contact allows us to estimate the critical shear stress of homogeneous dislocation nucleation. Within this isotropic approximation, the experimental results are in good agreement with the theoretical estimations. The density of preexisting dislocations determines a maximum tip radius of the indenter. This explains why the pop-in effect is found normally only in nanoindentation experiments.

\*Electronic address: leipner@cmat.uni-halle.de

<sup>1</sup>M. Göken and M. Kempf, *Z. Metallkd.* **92**, 1061 (2001).

<sup>2</sup>W. W. Gerberich, S. K. Venkataraman, H. Huang, S. E. Harvey, and D. L. Kohlstedt, *Acta Mater.* **43**, 1569 (1995).

<sup>3</sup>S. Suresh, T.-G. Nieh, and B. W. Choi, *Scr. Mater.* **41**, 951 (1999).

<sup>4</sup>J. D. Kiely, K. F. Jarausch, J. E. Houston, and P. E. Russell, *J. Mater. Res.* **14**, 2219 (1999).

<sup>5</sup>J. Li, K. J. Van Vliet, T. Zhu, S. Yip, and S. Suresh, *Nature (London)* **418**, 307 (2002).

<sup>6</sup>C. L. Kelchner, S. J. Plimpton, and J. C. Hamilton, *Phys. Rev. B* **58**, 11 085 (1998).

<sup>7</sup>J. A. Zimmerman, C. L. Kelchner, P. A. Klein, J. C. Hamilton, and S. M. Foiles, *Phys. Rev. Lett.* **87**, 165507 (2001).

<sup>8</sup>A. Gouldstone, K. J. Van Vliet, and S. Suresh, *Nature (London)* **411**, 656 (2001).

<sup>9</sup>T. F. Page, L. Riester, and S. V. Hainsworth, in *Fundamentals of Nanoindentation and Nanotribology*, edited by N. R. Moody *et al.*, Mater. Res. Soc. Symp. Proc. No. 522 (Materials Research Society, Pittsburgh, 1998), p. 113.

<sup>10</sup>E. Le Bourhis and G. Patriarche, *Philos. Mag. Lett.* **79**, 805 (1999).

<sup>11</sup>H. S. Leipner, D. Lorenz, A. Zeckzer, and P. Grau, *Phys. Status Solidi A* **183**, R4 (2001).

<sup>12</sup>T. F. Page, G. M. Pharr, J. C. Hay, W. C. Oliver, B. Lucas, E. Herbert, and L. Riester, in *Fundamentals of Nanoindentation and Nanotribology*, edited by N. R. Moody *et al.*, Mater. Res. Soc. Symp. Proc. No. 522 (Materials Research Society, Pittsburgh, 1998), p. 53.

<sup>13</sup>T. A. Michalske and J. E. Houston, *Acta Mater.* **46**, 391 (1998).

<sup>14</sup>D. F. Bahr, D. E. Kramer, and W. W. Gerberich, *Acta Mater.* **46**, 3605 (1998).

<sup>15</sup>B. R. Lawn, *J. Am. Ceram. Soc.* **81**, 1977 (1998).

<sup>16</sup>A. Kailer, Y. G. Gogotsi, and K. G. Nickel, *J. Appl. Phys.* **81**, 3057 (1997).

<sup>17</sup>A. B. Mann, D. van Heerden, J. B. Pethica, P. Bowes, and T. P. Weihs, *Philos. Mag. A* **82**, 1921 (2002).

<sup>18</sup>P. Feltham and R. Banerjee, *J. Mater. Sci.* **27**, 1626 (1992).

<sup>19</sup>J. P. Hirth and J. Lothe, *Theory of Dislocations* (Wiley, New York, 1982).

<sup>20</sup>J. Schreiber, L. Höring, H. Uniewski, S. Hildebrandt, and H. S. Leipner, *Phys. Status Solidi A* **171**, 89 (1999).